Heavy-ion-beam–induced hydrodynamic effects in solid targets

N. A. Tahir and D. H. H. Hoffmann
Institut für Kernphysik, Technische Universität Darmstadt, Schlossgarten Strasse 9, 64289 Darmstadt, Germany

J. A. Maruhn
Institut für Theoretische Physik, Universität Frankfurt, Postfach 11 19 32, 60054 Frankfurt, Germany

P. Spiller and R. Bock
Gesellschaft für Schwerionenforschung, Planckstrasse 1, 64291 Darmstadt, Germany
(Received 13 April 1999; revised manuscript received 24 May 1999)

It is expected that after the completion of a new high current injector, the heavy-ion synchrotron (SIS) at the Gesellschaft für Schwerionforschung (GSI) Darmstadt will accelerate U^{+28} ions to energies of the order of 200 MeV/u. The use of a powerful rf buncher will reduce the pulse length to about 50 ns, and employment of a multiturn injection scheme will provide 2×10^{11} particles in the beam that correspond to a total energy of the order of 1 kJ. This upgrade of the SIS, hopefully, will be completed by the end of the year 2001. These beam parameters lead to a specific power deposition of the order of 1–2 TW/g in solid matter that will provide temperatures of about 10 eV. Such low specific power deposition will induce hydrodynamic effects in solid materials, and one may design appropriate beam-target interaction experiments that could be used to investigate the equation of state of matter under extreme conditions. The purpose of this paper is to propose suitable target designs with optimized parameters for the future GSI experiments with the help of one and two-dimensional hydrodynamic simulations. Cylindrical geometry is the natural geometry for highly focused ion beams, and therefore cylindrical targets are the most appropriate for this type of interaction experiments. The numerical simulations presented in this paper show that one can experimentally measure the characteristic sound speed in beam heated targets which is an important physical parameter. Moreover, one can study the propagation of ion-beam-induced shock waves in the solid materials. Different values for the specific power deposition, namely, 10, 25, 50, and 100 kJ/g, have been used. In some cases the pulse length is assumed to be 40 ns while in others it is considered to be 50 ns. Various materials including lead, aluminum, and solid neon have been used. [S1063-651X(99)04410-4]

PACS number(s): 51.50.+v, 51.60.+a, 51.70.+f

I. INTRODUCTION

Compressed and highly focused heavy-ion bunches are an excellent tool for generating dense plasmas in solid state matter. Such heavy-ion bunches may carry terawatts of power, and can heat extended volumes of solid targets with a high stopping power that is proportional to Z^2, where Z is the effective charge of the projectile ion. The total power carried by a single heavy-ion bunch is given by the kinetic energy of the beam, T, times the total number of ions in the bunch, N, divided by the final duration of the pulse τ_f.

The heavy-ion synchrotron facility, the SIS, at the Gesellschaft für Schwerionenforschung (GSI), Darmstadt, is a unique facility worldwide that is capable of generating intense beams of energetic heavy ions. At present, the SIS can accelerate ions of Ar^{+18} to energies of about 300 MeV/u. Theoretically, the space charge limit for these ions allows acceleration of a maximum number of 3×10^{11} ions in a single beam, although the beam consisted of about 2×10^{10} particles in most of the experiments performed so far [1–3]. The pulse duration is of the order of 200–300 ns, while the beam spot radius is approximately 0.4 mm. These beam parameters lead to a specific energy deposition of the order of 1 kJ/g in solid matter.

It is expected that after the completion of the SIS upgrade that includes the introduction of a new high current injector and a powerful rf buncher, the SIS will be able to accelerate U^{+28} ions with energies up to 200 MeV/u that will be delivered in pulses that would be about 50 ns long. Employment of a multiturn injection scheme will provide about 2×10^{11} particles in the beam that will correspond to about 1.5-kJ total energy. This upgrading will hopefully be completed by the end of the year 2001. The above beam parameters correspond to a specific energy deposition, E_s of the order of 50–100 kJ/g in solid matter that corresponds to a specific power deposition of 1–2 TW/g. Numerical simulations predict [4] that specific power deposition in this range would produce temperatures of the order of 10–20 eV in solid matter.

Figure 1 shows the achievable matter temperature as a function of the specific power deposition highlighting various physics regimes that may be accessible with these parameters. It is seen that the SIS beam parameters that will be available in the near future would induce pure hydrodynamic effects in the targets. One should therefore design suitable beam-target experiments to investigate these hydrodynamic effects that can make very useful contribution to, for example, our knowledge of the equation of state of matter under extreme conditions. It has also been shown with the help of computer simulations that implosion of multilayered cylindrical targets using the SIS beam may lead to physical conditions required to create metallic hydrogen [5].

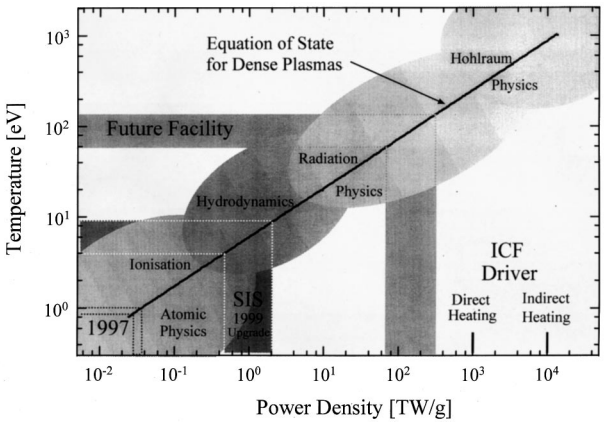

FIG. 1. Temperature as a function of specific power deposition.

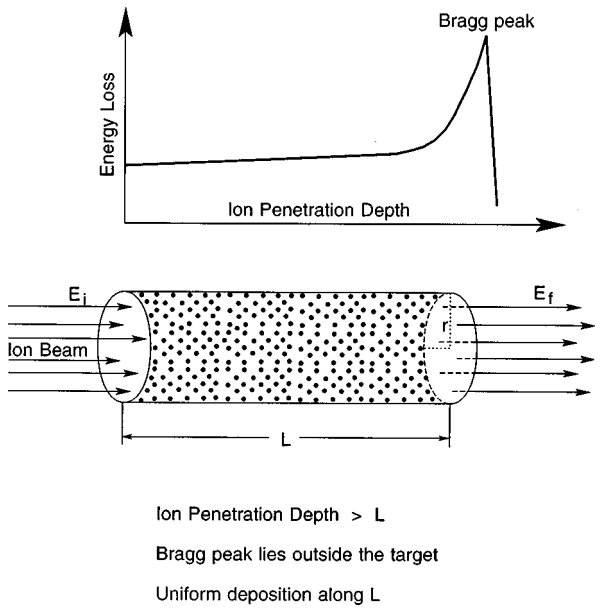

FIG. 2. A schematic presentation of ion beam-target interaction.

It is well known that during the past three decades, substantial progress has been made in the field of laser development. At present, there exist a number of laser systems that can deliver energy in the range of tens of kilojoule. In the next few years, laser systems capable of delivering energy in a megajoule range will become operational. For example, the National Ignition Facility project in the United States and a similar project in France will be completed within the next decade. One may therefore wonder why should one be interested in a comparatively very small heavy ion machine that can deliver energy in the range of a kilojoule? The answer to this question has a number of aspects, as discussed below.

First we note that there is a tremendous difference between the manner in which lasers and ion beams interact with matter. The laser heating of a solid target is basically a surface heating phenomenon that generates an outward expanding blowoff plasma. The laser light penetrates up to the critical density surface (where the plasma frequency becomes equal to the laser frequency), and there it is stopped. The laser energy is absorbed in the underdense region and at the critical density surface, and is transported into the overdense region via transport mechanisms including electron thermal conductivity, fast electron transport, and radiation transport that maintains the process of ablation at the ablation surface. Sharp density, temperature, and pressure gradients exist between the absorption region and the ablation surface. As a consequence, laser-produced plasmas are highly non-steady-state systems.

Ion beams, on the other hand, penetrate deep into solid matter, and their penetration depth is determined by the initial ion energy and the physical state of the target material. Ion beams therefore heat extended volumes of matter and thus generate solid density plasmas. If the ion energy and the target dimensions are adjusted in such a manner that the ion range is longer than the target length, the Bragg peak will then lie outside the target and the energy deposition will be almost uniform along the cylinder length that in turn will uniformly heat the target, as is shown schematically in Fig. 2. Ion beams therefore generate extended volumes of steady-state solid density plasmas. Such a system is much more attractive for doing basic physics experiments including energy loss of energetic ions in ionized matter [6–10] and equation-of-state studies of strongly coupled plasmas [11–13].

Second, it is generally accepted that due to its large efficiency and high repetition rate, a heavy-ion driver is much more suitable compared to a laser to drive a future power plant based on an inertial confinement fusion (ICF) scheme. It is therefore very important that we learn as much as possible about ion-beam-generated plasmas.

This paper presents one- and two-dimensional numerical simulations of the hydrodynamic response of solid cylindrical targets irradiated by heavy-ion beams. It is seen that using a suitable beam-target configuration (the beam radius is significantly less than the target radius), one may study the propagation of heavy-ion-induced shock waves along the target radius. An experimental measurement of the kinematic parameters of these shock waves, including the velocity of the shock front and the velocity of matter behind the shock, would allow one to determine the thermodynamic characteristics and hence the equation of state of the hot dense matter. This will be a useful contribution to this field. Using a different configuration in which the beam radius is equal to the target radius so that the cylinder is uniformly heated, one may measure the speed of the rarefaction wave moving from the cylinder surface toward the radius. The speed with which this rarefaction wave travels is in fact the characteristic sound speed in the material that one should be able to measure directly in the experiments.

Section II discusses the problem of generating intense beams of energetic heavy ions and highlights the important features of the GSI heavy-ion synchrotron. Section III discusses the basic range-energy relations for energetic ions allowing estimation of specific energy deposition E_s and specific power deposition P_s by various ion species in different materials. The different computer codes used to carry out the simulations presented in this paper are briefly described in Sec. IV, while the simulation results are presented in Sec. V. Conclusions drawn from this work are noted in Sec. VI.

II. GENERATION OF HIGH POWER ENERGETIC HEAVY-ION BEAMS

The generation of intense heavy-ion beams is strongly connected to space charge effects which may dominate the

beam dynamics in the accelerator significantly. Therefore, to keep the space charge effects as small as possible, lower charge states of heavy projectiles, with a high A/Z relation are required, where A is the atomic mass of the projectile ion. This may lead to a high ion magnetic rigidity that is given by

$$B\rho = A/Z(1/c)\sqrt{T^2 + 2Tm_u c^2},$$

where T is the beam kinetic energy in eV/u, m_u is the mass of a nucleon in kg, and c is the speed of light. Hence in order to be able to generate intense beams of energetic heavy ions, the accelerators must have the capability to handle such high rigidity ions.

Various concepts for appropriate accelerator facilities already exist. One of the important goals of this field of research is to design an accelerator that can deliver a beam with sufficient power to drive an ICF target. Recently, such an accelerator design together with design for a corresponding ignition facility has been worked out by a European study group with GSI as the coordinating institute (HIDIF [14]). This European approach was based on a 6-km long linac and an advanced storage ring system with external induction bunchers. Using a Bi^{+1} beam, a possible operation rigidity was found to be 210 Tm. The aim of such an accelerator facility is to deliver 6-MJ beam energy in a pulse of 6 ns to the converters of an indirect drive inertial fusion target.

GSI also provides a unique possibility to perform experiments with heavy-ion-beam-induced dense plasma [1–3]. The maximum in terms of energy deposition could be achieved by focusing a single Ar-ion bunch of 2×10^{10} particles with a kinetic energy of 300 MeV/u down to a spot radius of 350 μm. With an achieved specific energy deposition of about 1 kJ/g and a pulse duration of about 300 ns, a lead target could be heated up to a temperature of about 1 eV [4].

In order to provide better conditions for this type of experiments, a new high current injector [15] is being set up within the the framework of GSI's high current project. The new injector which consists of RFQ (radio frequency quadrupole) and IH (interdigital H-mode) structures will replace by the end of 1999 the old WIDEROE structure at the front end of the UNILAC (Universal Linear Accelerator). This injector has the capability to accelerate a low charged uranium beam U^{+4} of up to 15 emA to an energy of 1.4 MeV/u. By the interaction with a gas jet target, it is then possible to enhance the charge state of the projectiles to up to a charge state of +28. This higher charge state is required in order to reduce the rigidity of the beam for the injection in the heavy ion synchrotron SIS. By multiturn injection in the SIS the UNILAC current will be enhanced by a factor of up to 20. Thus at a SIS ring circumference of 216 m and with a typical injection energy of 11.4 MeV/u, a coasting beam with 2×10^{11} uranium ions can be expected. This number of particles matches the transverse space charge limit given by the incoherent tune shift dQ (Laslett tune shift) after rf capturing:

$$dQ_v = (Z^2/A)Nf_1 r_p/(\beta^2\gamma^3 Bf(\epsilon_h + \sqrt{\epsilon_h \epsilon_v}),$$

where f_1 is a form factor for the transverse distribution function, r_p is the proton radius, $\beta = v/c$, γ is the Lorenz factor, Bf is the bunching factor ($\approx$0.4), and ϵ_v and ϵ_h are the horizontal and vertical beam emittances, respectively. With the transverse emittances of the beam after injection being $\epsilon_h = 200$ mm mrad and $\epsilon_v = 50$ mm mrad, the incoherent tune shift was calculated to be $dQ_v \leqslant 0.35$. However, in order to avoid crossing of systemic resonances of first and second order due to the space charge tune depression, the working points (Q values) have to be chosen carefully.

The longitudinal stability of the beam is maintained unless the space charge coupling with the conductive wall of the beam tube or with narrow or wide band impedances of crucial devices like kicker magnets or rf cavities does not excite strong oscillations within the beam. A basic criterion which slightly overestimates this effect, is given by the Keil-Schnell limit

$$I_c < (A/Z)2(dp/p^2)(m_u c^2/e)\beta^2\gamma\eta_{\mathrm{Trans}}/[(Z_n/n)f_2],$$

where I_c is the coasting beam current, dp/p the momentum spread, η_{Trans} the frequency slip factor, Z_n/n the impedance, and f_2 a distribution form factor. The total impedance consisting of a real and an imaginary space charge contribution can be approximated by

$$Z_n/n = R_n/n + iX_n/n \text{ with } X_n/n \approx -377/[2\beta\gamma^2(1 + 2\ln(r_{\mathrm{tube}}/r_{\mathrm{bean}}))].$$

In the above equations, $r_{\mathrm{tube}}/r_{\mathrm{beam}}$ is the ratio between the tube radius and the beam radius. This stability threshold depends on the specific distribution function [16], and can be exceeded by a factor of up to 10, depending on the strength of the resistive part R_n of the total impedence. In any case, immediate bunching and acceleration after injection, is useful to avoid a growth of the longitudinal phase space. At a momentum spread of 5×10^{-4} of the coasting beam, we expect to exceed the Keil-Schnell limit by a factor of 7.

Since the longitudinal and transverse space charge limits become most crucial at lower beam energies, the maximum number of particles in the relevant phase space area is defined by the conditions after injection. In other words, there are severe limits on the minimum phase space volume of the beam at a given number of particles. This six-dimensional (6D) phase space volume is defined according to the mentioned limitations by the horizontal and vertical emittances $\epsilon_{h/v}$ and the beam length z times the momentum spread dp/p longitudinally. Unfortunately, the size of this phase space volume has a major impact on the transverse focusibility as well as on the longitudinal compressibility after acceleration.

Nevertheless, a possible way to achieve a multiplication of the total beam power on the target is to subdivide the initial longitudinal phase space area in a number of separate smaller phase spaces, or, in other words, to work with a large number of individual bunches. Such a concept was taken into account in the HIBALL [17] and the HIDIF study [14]. Since the individual bunches have to arrive at the target position at the same time, and therefore a delay line system is required for synchronization. Another option is to place the target into the center of the ring and to use a number of beam lines guiding the bunches from a number of extraction points from the circumference to the center.

If only one beam line to the target is available, as in the GSI accelerator facility, one has to capture the total number of particles in a single bunch. Since the acceleration in the SIS18 takes place at the fourth harmonic of the revolution

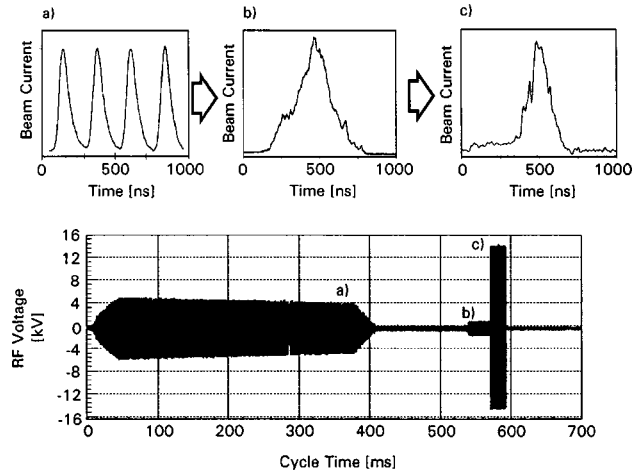

FIG. 3. Measured bunch current signals at different stages of the acceleration cycle together with the measured rf gap voltage over the modified acceleration process in the SIS. Shown are (a) the typical four bunch structure after acceleration at harmonic $h=4$, (b) a single bunch profile after adiabatic debunching and rebunching at $h=1$, and (c) a single bunch after fast bunch compression.

frequency, a special operation mode for the generation of such a single bunch was invented in March 1997. The applied scheme is based on a debunching and rebunching of the beam after acceleration. The disadvantage of this scheme is that the beam is very sensitive to longitudinal instabilities after debunching. In this phase of a coasting beam the momentum spread is small, and a high shunt impedance of the rf cavities in the ring may cause a filamentation of the longitudinal phase space. Therefore, for the future high current operation of the SIS18 with U^{+28} beams, a maximum shunt impedance of the cavities of <1 kΩ can be tolerated. Eventually a longitudinal feed back system has to be installed, which may have the capability to reduce the present impedance by up to a factor of 10.

In any case, for the final compression, a voltage-jump-induced phase space rotation has to be applied. This concept of fast compression could be studied within a number of machine experiments, and has already been employed for the generation of short bunches for plasma physics experiments at GSI [18]. The evolution of the beam current over the entire acceleration cycle in the SIS is shown in Fig. 3. The final bunch length τ_f after compression is determined by the square root of the ratio between initial to final rf-voltage amplitude:

$$\tau_f=\sqrt{V_i/V_f}\,\tau_i=[(dp/p)_i/(dp/p)_f]\tau_i.$$

In order to provide a sufficiently high compression voltage V_f, GSI has launched a project for the set-up of a dedicated bunch compressor cavity. This new type of magnetic alloy cavity will provide an rf-amplitude of 200 kV for a compression at a fixed frequency of 1 MHz.

The principal restrictions for the longitudinal compression after acceleration are given by the maximum momentum spread and emittance which can be tolerated by the ring lattice and the transport and focusing system. This is mainly due to the dispersion function D-related growth of the beam radius $r_{\mathrm{beam}}=\sqrt{\beta_x\epsilon+(Ddp/p)^2}$ (β_x being the local transverse beta function) and in addition by the growth of the focal spot diameter due to second order image aberrations [19]. These effects restrict the final momentum spread to $(dp/p)_f \leqslant \pm 1\%$. Thus, assuming the smallest possible longitudinal emittance defined by the stability criteria at injection, the minimum bunch length on the target is already defined under the assumption of phase space conservation. Considering a typical coasting beam momentum spread of $\pm 5\times 10^{-4}$ after acceleration, a compression down to a bunch length of 50 ns will be possible [20] with the new bunch compressor cavity.

In a first order approximation the minimum spot radius r on the target is given by the beam convergence α behind the final focusing lens and the emittance ϵ of the beam as $r=\epsilon/\alpha$. Strong focusing systems are required in order to achieve a focusing angle as steep as possible and to minimize the spot size. Currently two kinds of strong focusing systems are available at the high temperature experimental area at GSI: a quadrupole focusing system based on conventional warm iron magnets [21], and a plasma lens which was developed at GSI [22] for this purpose. With these systems, beams with a neglectible momentum spread but relatively large emittance ($\approx$40 mm mrad) can be focused down to a spot radius of 350 μm. However, at a momentum spread of $\pm 1\%$ the effective spot radius will grow by image aberrations to about 1 mm.

Taking into account the above beam parameters, GSI will be able to provide, in the year 2002, uranium beams with a total power of about 40 GW for plasma physics experiments. These bunches will deposit a specific power of about 1–2 TW/g in a solid target. Numerical simulations predict that with these values of the specific power deposition, one may be able to achieve temperatures of the order of 10–20 eV in solid matter [4].

III. RANGE-ENERGY RELATIONS FOR ENERGETIC IONS AND ESTIMATION OF SPECIFIC POWER DEPOSITION BY THE SIS BEAM IN SOLID MATTER

The specific power deposited by a collimated beam of energetic ions in matter is defined by

$$P_s=E_s/\tau, \tag{1}$$

where τ is the pulse duration and E_s is the specific energy deposition given by

$$E_s=[dE/d(\rho x)]N/(\pi r^2). \tag{2}$$

In the above equation N is the total number of particles in the beam, r is the radius of the beam spot, and $dE/d(\rho x)$ is the usual energy loss term.

If one arranges the ion energy and the target dimensions in such a manner that the ion range is larger than the target length, the Bragg peak will lie outside the target and the energy will be deposited almost uniformly along the cylinder. In such a case one may approximately write

$$dE/d(\rho x)=E/(\rho R), \tag{3}$$

where E is the initial ion energy, ρ is the material density, and R is the ion range.

Using the above equations we have estimated the specific energy and the specific power deposition by a uranium beam with an ion energy of 200 MeV/u in solid lead. The total number of ions in the beam is assumed to be 2×10^{11}, and the pulse duration is considered to be 50 ns. The beam spot radius is assumed to be 1.0 mm, while the ion range in solid lead is calculated using the TRIM code [23]. Our calculations show that the beam with above parameters will deposit a specific energy deposition of about 30 kJ/g and a specific power deposition of approximately 0.6 TW/g in a solid lead target.

IV. A DESCRIPTION OF HYDRODYNAMIC SIMULATION MODELS

This section describes the updated version [24,25] of the one-dimensional computer code MEDUSA [26] and the two-dimensional hydrodynamic code MULTI-2D [27] that have been employed to carry out these simulations.

A. Computer code MEDUSA

The original version [26] of the MEDUSA code is a one-dimensional, two-temperature simulation model with Lagrangian hydrodynamics. It can handle spherical, cylindrical, and plane geometries. It was basically written to simulate laser-driven compression of solid deuterium-tritium (DT) microspheres. It assumes an ideal gas equation of state (EOS) for ions as well as for the electrons, and that electron and ion thermal conduction is the only means of energy transport in the target. It does not include radiation or superathermal electron transport. This program was previously modified [28] to allow for ion-beam-driven implosion of sophisticated multilayered reactor-size targets. Radiation transfer effects were included using a diffusion approximation (a three-temperature model). This version of the code known as MEDUSA-KAT [24,25], also includes analytically fitted Los Alamos EOS data from the SESAME library for the electrons.

In the experiments to be performed at the GSI, the target temperature will be very low (10–20 eV) compared to that in ICF plasmas (300 eV in the compression phase and 100 keV in the burn phase). One may therefore completely neglect the radiation effects in the former case, and one would not require a three-temperature model. In fact a one-temperature model representing the matter temperature will be sufficient. The electron and ion thermal conductivities will also not play an important role in these experiments. Moreover, the accuracy of the analytic fits to the SESAME data is also questionable at such low temperatures. In order to take care of these problems, the MEDUSA code has been modified to a one-temperature model, and the EOS variables are evaluated by direct interpolation of the SESAME data tables. This version of the code has been exclusively developed to simulate the future heavy-ion-matter experiments at the GSI, and we call it MEDUSA-GSI for future reference.

B. Computer code MULTI-2D

The code MULTI-2D [27] solves hydrodynamics and radiation transport in axial geometry. It uses an unstructured Lagrangian grid based on triangles, and includes facilities for tabulated equations of state. There is only one temperature, and thermoconductivity, although included in the code, was not used for the simulations presented here. The beam deposition is treated by following a large number of beamlets through the grid and depositing their energy locally. For the present studies, radiation transport was neglected, and the equation of state for lead was taken from the Los Alamos SESAME EOS data library.

The target temperature with the beam parameters considered in this study will be of the order of 10 eV. It is therefore a reasonable approximation to use the ion stopping power model that is valid for the cold matter to calculate the ion range in the target. This model includes the excitation and ionization of the bound target electrons through Coulomb interaction with the incident ions. These processes can be treated by the Bethe formula [29], that, however, is valid only at high energies. At low energies, shell corrections are introduced. At very low energies, even with shell corrections, the Bethe formula is not valid. In such a case the Linhardt LSS (Lindhart, Scharff, and Schott) model [30] is applied. In this model a Thomas-Fermi description of the bound electrons is used, and the stopping power due to excitation and ionization of the electrons is added to a contribution from nuclear elastic scattering of the incident ions that becomes important at such low energies. The value of the effective charge of the incident ion may be calculated using the formula provided in Ref. [31].

V. NUMERICAL SIMULATION RESULTS OF BEAM-TARGET INTERACTION

This section presents numerical simulation results of the hydrodynamic response of heavy-ion-beam heated solid cylindrical targets. The relevance of these simulation results to the future experiments to be done at the GSI has also been discussed. The beam-target geometry is arranged in such a manner that the ions are incident on one face of the cylinder while the initial ion energy and the target dimensions are so adjusted that the ion penetration depth is larger than the cylinder length. The ions will then lose a part of their energy in the target, and emerge from the opposite face of the cylinder with a substantially reduced energy. The Bragg peak would then lie outside the target (see Fig. 2), and the energy deposition along the projectile path (cylinder length) would be fairly uniform. If the cylinder length is a few times larger than its radius, this problem could be approximated to a one-dimensional hydrodynamic expansion (compression) along the radius. In order to check the validity of this assumption, typical calculations have been carried out using a two-dimensional hydrodynamic computer code MULTI-2D [27].

A. Shock wave propagation in solid matter

The proposed beam-target geometry for this type of experiments is shown in Fig. 4. The target consists of a solid cylinder with a radius, R_c, and has a length L, while the ion beam is focused on the left face of the cylinder. The beam has a Gaussian deposition profile along the radius, and a power function is given by

$$P(r)=P_0\exp[-r^2/(2\sigma^2)], \tag{4}$$

where the symbols have their usual meaning.

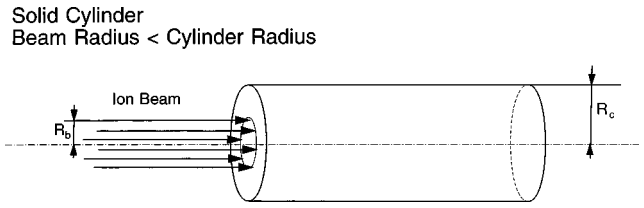

FIG. 4. Beam-target configuration suitable for ion-beam-induced shock wave studies (the beam radius is less than target radius).

TABLE I. Sound speed in uniformly heated solid density lead cylinder.

Specific energy kJ/g	Temperature (eV)	Pressure (Mbar)	Sound speed (km/s)
10	3.70	0.85	3.60
25	6.40	1.60	5.00
50	9.50	2.80	6.40
100	14.50	4.85	8.30

In such a case the beam would effectively heat the material that lies within the full width at half maximum (FWHM) of the Gaussian distribution, and one may consider this as the effective beam radius R_b. By considering R_c to be greater than R_b, a cylinder of heated matter may be created with a radius R_b that is surrounded by a shell of solid cold matter having a thickness of $R_c - R_b$. The pressure in the hot zone would increase substantially, which would launch a shock wave in the surrounding cold material and which will propagate outwards along the radius. One can study the characteristics of such shock waves in actual experiments that may be very useful for equation-of-state investigations of matter under extreme conditions. We have carried out an extensive simulation study of the hydrodynamic behavior of solid cylindrical beam-heated targets made of different materials including lead, aluminum, neon, and hydrogen. In the present paper we however report results from lead targets only.

According to the TRIM code [23], the range of 200-MeV uraniumions in cold solid lead is about 1.7 mm. In order to allow for a uniform energy deposition in the target, it is assumed that the target length is 1.5 mm. The target radius is considered to be 3.0 mm. It is assumed that the FWHM of the ion deposition profile is 0.5 mm, so that the length of the cylinder of the heated material is three times its radius, and the one-dimensional approximation is applicable to this problem. In order to check the accuracy of this assumption in the case of this target with the given beem parameters, calculations have been performed using the two-dimensional hydrodynamic code MULTI-2D [27]. The specific energy deposition in the target is assumed to be 50 kJ/g, while the pulse length is considered to be 50 ns. Figures 5(a)–5(c) present two-dimensional density plots of this target (on a radius-axis plane) at different times after the pulse has delivered its energy to the target. Figure 5(a) is plotted at $t = 50$ ns, which is the time when the pulse has just been switched off. It is seen that a shock wave has started to

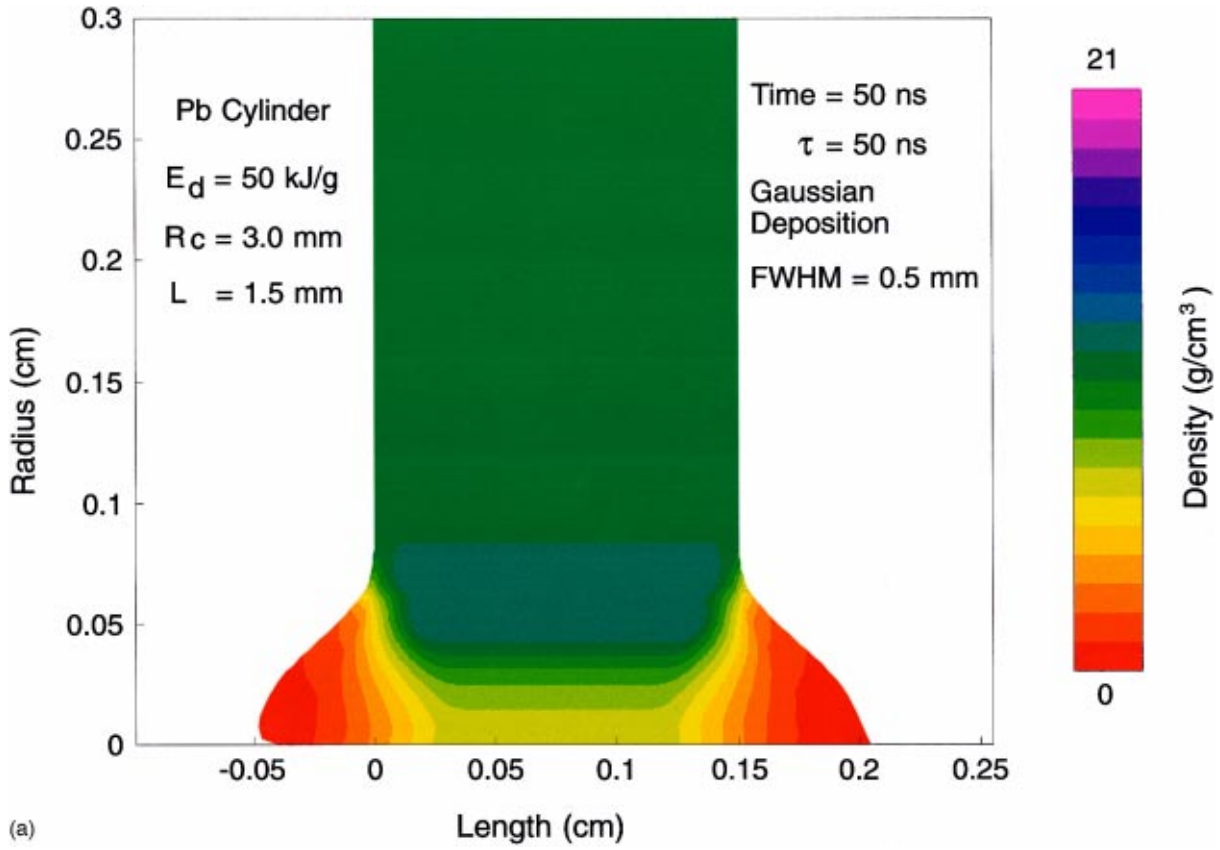

FIG. 5. (Color). (a) Target density on a radius-axis plane for a lead target at $t = 50$ ns using a specific power deposition of 50 kJ/g, pulse length of 50 ns, a Gaussian deposition profile along the radius with a FWHM of 0.5 mm, a target length of 1.5 mm, and a target radius of 3 mm (2D calculations using the MULTI-2D code). (b) Same as in (a), but at $t = 150$ ns. (c) Same as in (a), but at $t = 300$ ns.

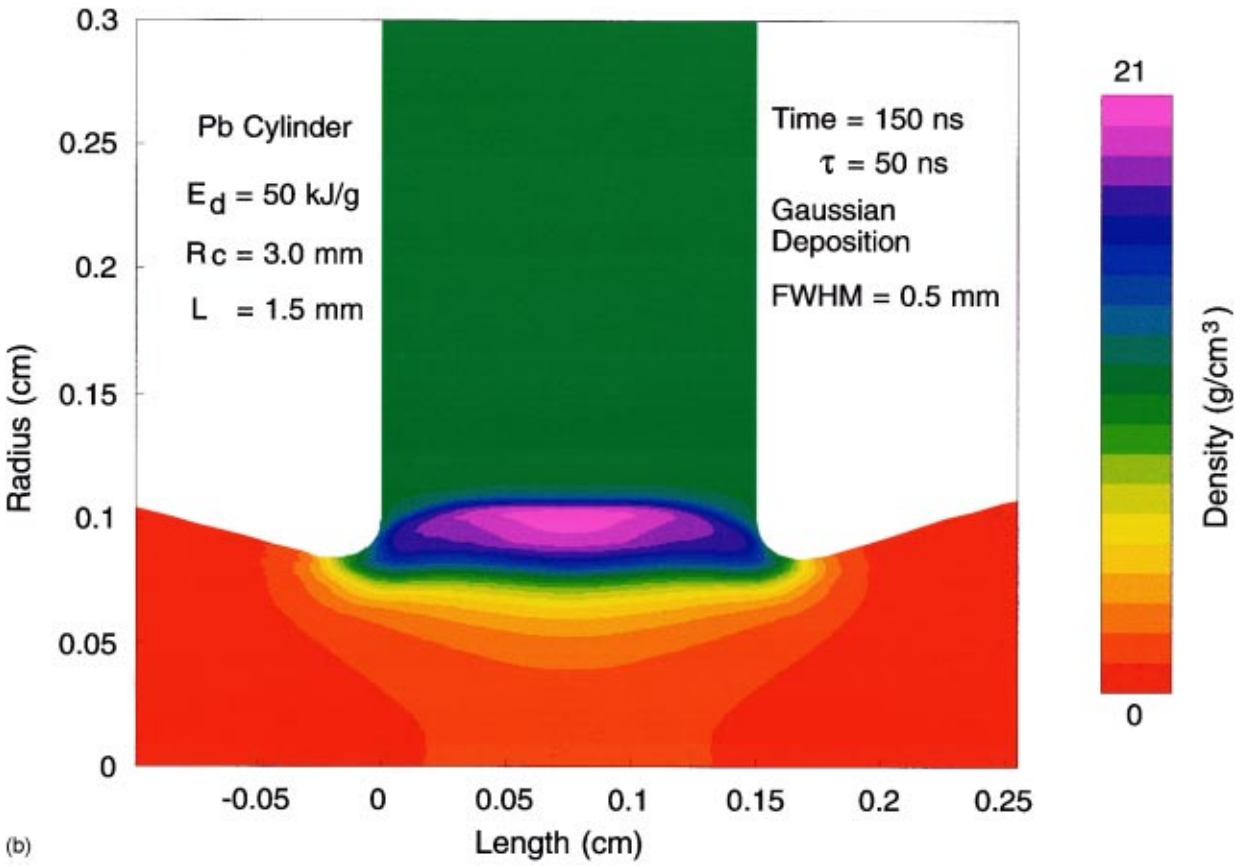

(b)

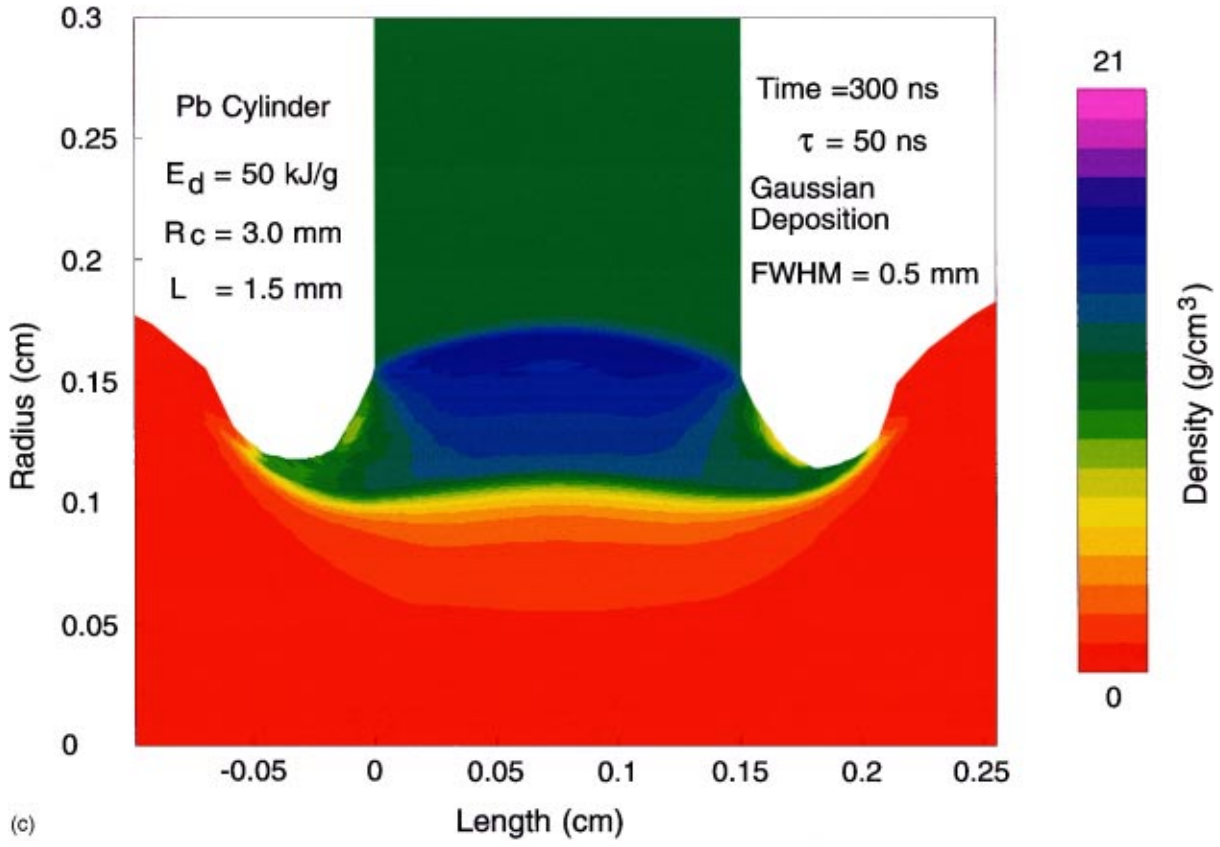

(c)

FIG. 5 (*Continued*).

develop at the boundary of the hot and cold material. Figure 5(b) shows that, at $t=150$ ns, the shock has propagated to a position $r=1.0$ mm, and the density in the shock region is about 21 g/cm^3. Figure 5(c) indicates that, at $t=300$ ns, the shock has moved to a position $r=1.75$ mm while the density in the shock region has been significantly reduced. These figures show very clearly that although there is a considerable expansion of the material along the cylinder axis in the beam-heated region, there is hardly any expansion of the cold shock compressed region along the cylinder axis. As a matter of fact the shock maintains its profile even at a very long time after the pulse is switched off, namely, $t=500$ ns. This beahvior suggests that it may be a reasonably good approximation to use a one-dimensional hydrodynamic computer code to carry out such calculations. The rest of the calculations presented in this paper have therefore been done using the one-dimensional code MEDUSA-GSI.

Simple calculations show that the SIS uranium beam will deposit a specific energy of the order of 25 kJ/g in solid lead. We have carried out a calculation using this value of E_s employing the one-dimensional simulation model MEDUSA-GSI. The results are presented in Figs. 6(a) and 6(b) where we plot the target density and pressure along the radius, respectively, at varius times. The cylinder radius in this case is considered to be 2.5 mm. It is seen from Fig. 6(a) that as the shock wave moves outward along the cylinder radius, the density in the shock region decreases because of the cylindrical geometry. As a consequence, the pressure also decreases as shown in Fig. 6(b). Since the propagation speed of the shock front is $\propto(P_1-P_0)^{1/2}$, where P_1 and P_0 represent the pressure behind the shock and in the unshocked medium, the shock wave is slowed down with time.

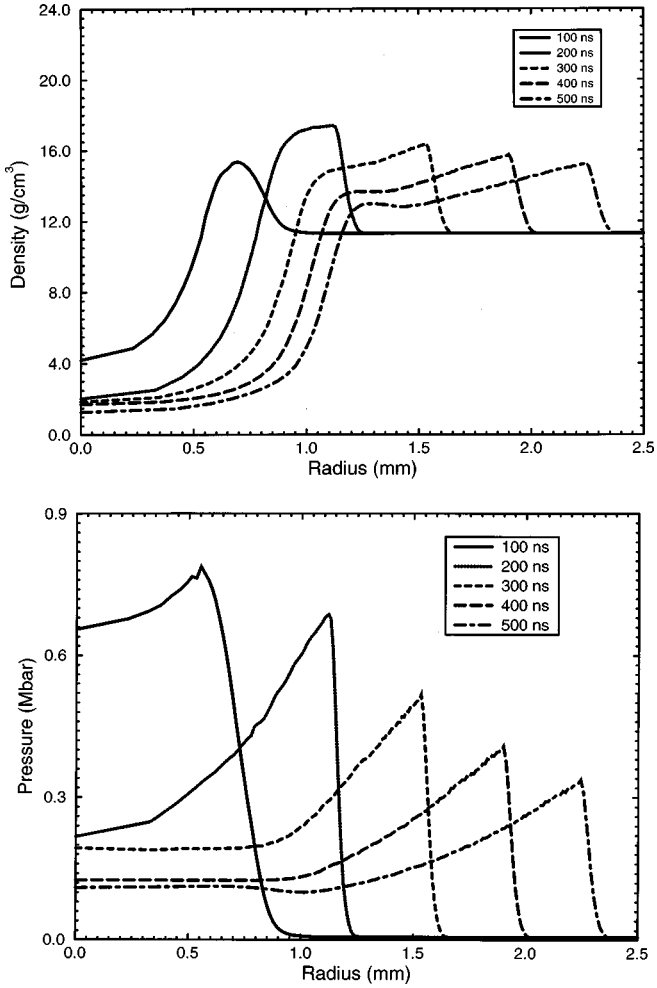

FIG. 6. (a) Density vs radius at different times for a Pb target using a specific energy deposition of 25 kJ/g, a pulse length of 50 ns, and a Gaussian deposition profile along the radius with a FWHM of 0.5 mm and a target radius of 2.5 mm (1D calculations using the MEDUSA code). (b) Corresponding pressure profiles for the case presented in (a).

B. Modeling of sound speed measurements in beam-target interaction experiments

The characteristic sound speed in a material under given physical conditions is a very important basic physical parameter. In many cases of interest it may be important to know this parameter with reasonable accuracy. For example, the confinement time of a small highly compressed inertial fusion spherical microsphere is given by

$$\tau=R/(4c_s),$$

where R is the radius of the target and c_s is the speed of sound. The factor 4 in the denominator appears because, in the case of a sphere, half of the mass lies within the outer 20% of the sphere radius and one may consider fusion to be over after the half of the mass has been disassembled.

From thermodynamic considerations the speed of sound is given by

$$c_s=[(\partial P/\partial\rho)_s]^{1/2})$$

where in the above equation the derivative of pressure with respect to density is evaluated at constant entropy S. One could therefore easily evaluate the sound speed from the equation of state data like the Los Alamos SESAME tables. However, the accuracy of such huge data tables cannot be guaranteed over the entire range of the physical parameters, as discussed in Sec. V A. Consequently, the accuracy of the calculations based on such data would also be questionable. It is thus important to have experimental measurements of the sound speed that will also confirm the validity or nonvalidity of the EOS data calculated theoretically.

A comparison was given in Ref. [12] between theoretical and experimental results, while the experiments have been performed creating extreme conditions in matter employing shock waves generated by chemical explosives. It is shown in this paper with the help of numerical simulations that one should be able to measure the sound speed in ion-beam-heated targets. The beam-target geometry is shown in Fig. 7. It is a cylindrical target that is uniformly heated along the radius as well as the axis. This could be accomplished by using an ion beam that does not have a Gaussian power deposition profile along its radius, but instead has a rectangular (uniform) profile. When the beam is switched off, a rarefaction wave will move from the target surface along its radius toward the axis. The speed with which this rarefaction wave will travel is the characteristic sound speed in the target material under the given physical conditions. Hence by measuring the speed of this rarefaction wave, one would measure the sound speed. This has been modeled with the help of

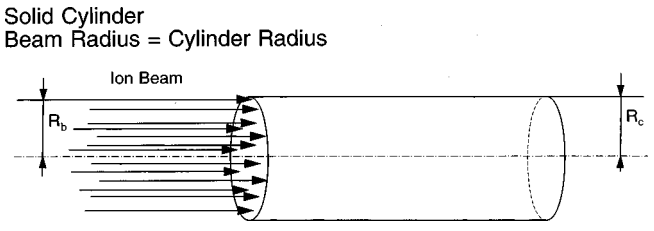

FIG. 7. Beam-target configuration suitable for sound speed measurement (the beam radius is equal to the target radius and the uniform energy deposition along radius).

numerical simulations, and the results are given below.

These calculations have been carried out using the one-dimensional computer code MEDUSA-GSI. A solid lead cylinder with a radius of 1 mm is irradiated by the ion beam, that also has a radius of 1 mm. The pulse length is assumed to be 40 ns while four different values for the specific energy density, namely, 10, 25, 50, and 100 kJ/g have been considered. In Fig. 8(a) we plot the pressure profiles vs the target radius for the above four cases of the specific power deposition at a time of 40 ns, when the beam has delivered its total energy. The corresponding temperature profiles are presented in Fig. 8(b). In Fig. 9, we show the density profiles vs target radius at different times for the case that uses a specific energy deposition of 25 kJ/g. This figure shows that this value of specific power deposition creates a temperature of about 6.4 eV and a pressure of 1.6 Mbar in solid lead. The speed of the rarefaction wave as calculated from the density profile is about 5 km/s, which is the speed of sound in solid lead at the above temperature and pressure. One should be able to measure the position of the rarefaction front as a function of time in the experiments, and thus calculate the speed of sound from this experimental data.

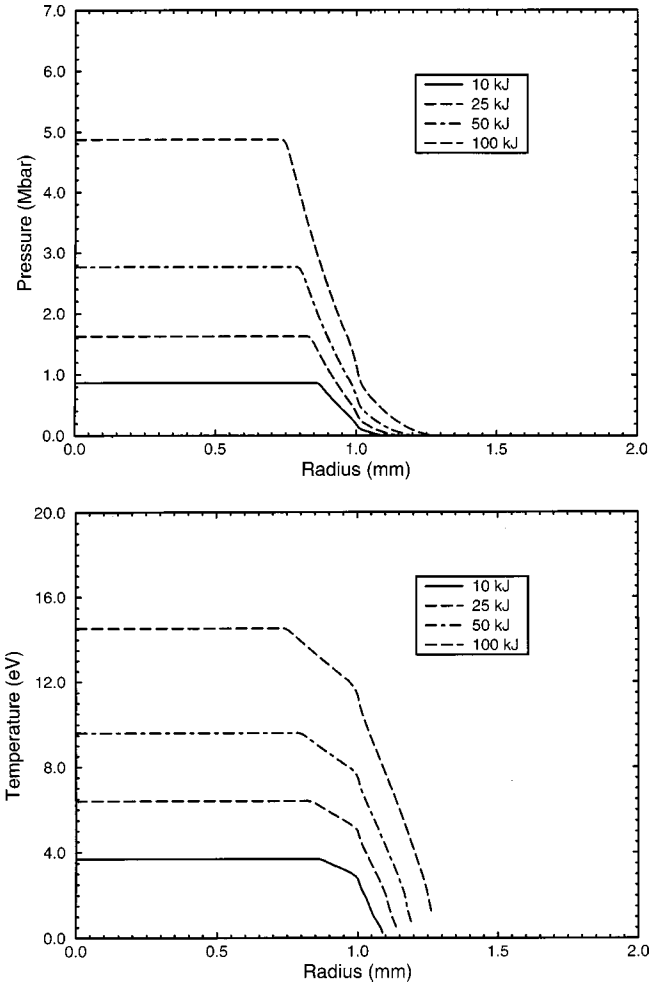

FIG. 8. (a) Pressure vs radius at $t=40$ ns in the case of a uniformly heated lead cylinder (see Fig. 7) using four different values of specific energy deposition assuming a pulse length of 40 ns, a beam radius of 1 mm, and a target radius of 1 mm. (b) Pressure profiles corresponding to the case shown in (a).

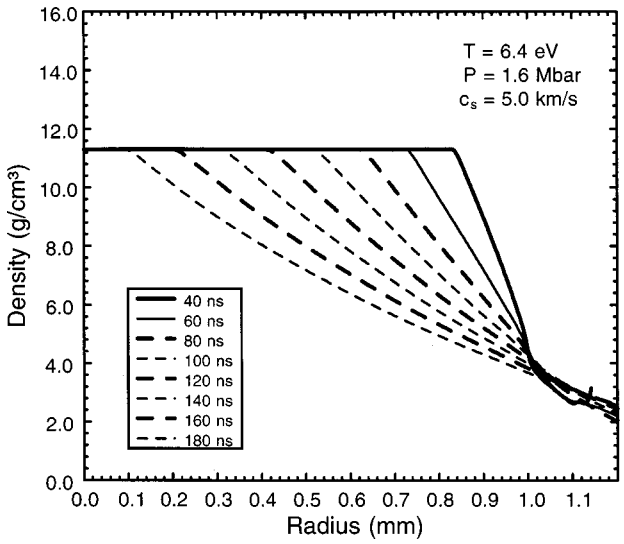

FIG. 9. Density vs radius in the case of a solid lead cylinder with a radius of 1 mm, and a beam radius of 1 mm, using a specific power deposition of 25 kJ/g and assuming a pulse length of 40 ns.

Table I presents the corresponding values of the parameters for other cases of specific power deposition. Using this technique, one may be able to measure the characteristic sound speed in other materials of interest.

VI. CONCLUSIONS

This paper presents a numerical modeling of proposed heavy-ion-matter experiments that could be performed at the upgraded heavy-ion synchrotron facility (SIS) at the GSI darmstadt. It is expected that after the completion of a new high current injector and a powerful rf-buncher, the SIS facility would accelerate intense beams of U^{+28} ions with an ion energy of the order of 200 MeV/u that will be delivered in pulses which will be 50 ns long. The total energy in the pulse will be about 1.5 kJ, and it will lead to a specific energy deposition of 50–100 kJ/g and a specific power deposition of 1–2 TW/g in solid matter. It is expected that this upgrade of the facility will be completed by the end of the year 2001.

The above beam parameters will lead to a temperature of about 10 eV in solid matter. This temperature regime is dominated by pure hydrodynamic effects, and one may design suitable beam-target experiments to study such phenomena that will help to measure the EOS parameters of different materials. This paper proposes appropriate target designs with parameters optimized according to the SIS beam parameters that may be used in future experiments at the SIS. It is

ing shown with the help of numerical simulations that shock waves can be generated in these targets by the ion beam and the kinematic parameters of these shock waves including propagation velocity of the shock front and the velocity of the material behind the shock wave could be measured experimentally. With the help of these shock parameters, one may easily determine the EOS parameters of these materials. The numerical simulations presented in this paper also show that one should be able to measure the sound speed in uniformly heated cylindrical targets with reasonable accuracy.

ACKNOWLEDGMENTS

The authors wish to thank the German Ministry of Research (BMBF) for providing financial assistance to carry out this work.

[1] S. Stöwe, R. Bock, M. Dornik, P. Spiller, M. Stetter, V. E. Vortov, V. Mintsev, M. Kulish, A. Shutov, V. Yakaushev, B. Sharkov, A. Golubev, B. Bruynetkin, U. Funk, M. Geißel, D. H. H. Hoffmann, and N. A. Tahir, Nucl. Instrum. Methods Phys. Res. A **415**, 61 (1998).
[2] U. Funk, R. Bock, M. Dornik, M. Geißel, M. Stetter, S. Stöwe, N. A. Tahir, and D. H. H. Hoffmann, Nucl. Instrum. Methods Phys. Res. A **415**, 68 (1998).
[3] C. Stöckel, O. Boine-Frankenheim, M. Geißel, M. Roth, H. Wetzler, W. Seeling, O. Iwase, P. Spiller, R. Bock, W. Süß, and D. H. H. Hoffmann, Nucl. Instrum. Methods Phys. Res. A **415**, 558 (1998).
[4] N. A. Tahir, D. H. H. Hoffmann, J. A. Maruhn, K.-J. Lutz, and R. Bock, Phys. Plasmas **5**, 4426 (1998).
[5] N. A. Tahir, D. H. H. Hoffmann, J. A. Maruhn, K.-J. Lutz, and R. Bock, Phys. Lett. A **249**, 489 (1998).
[6] C. Deutsch and G. Maynard, Phys. Rev. A **26**, 665 (1982).
[7] C. Deutsch, Ann. Phys. (N.Y.) **11**, 1 (1986).
[8] T. Mehlhorn, J. Appl. Phys. **52**, 6522 (1981).
[9] E. Nardi and Z. Zinamon, Phys. Rev. Lett. **49**, 1251 (1982).
[10] K. A. Long and N. A. Tahir, Phys. Rev. A **35**, 2631 (1987).
[11] H. Kitamura and S. Ichimaru, J. Phys. Soc. Jpn. **65**, 1250 (1996).
[12] A. V. Bushman and V. Fortov, *Wide-Range Equation of State for Matter Under Extreme Conditions*, Soviet Technical Review B, Thermonuclear Physics Vol. 1 (Harwood, London, 1987).
[13] R. Redmer, Phys. Rev. E **59**, 1073 (1999).
[14] The HIDIF-Study, GSI Report No. GSI-98-06 (1998).
[15] U. Ratzinger (unpublished).
[16] I. Hofmann, Laser Part. Beams **3**, 1 (1985).
[17] D. Böhne *et al.* Nucl. Eng. Des. **73**, 195 (1982).
[18] P. Spiller *et al.* (unpublished).
[19] P. Spiller and I. Hofmann, Nucl. Instrum. Methods A **415**, 384 (1998).
[20] P. Spiller and R. W. Müller, GSI Report No. GSI-96-07, ISSN 0171-4546 (1996).
[21] P. Spiller, GSI Report No. GSI-94-11 (1994).
[22] M. Stetter *et al.*, Nuovo Cimento A **106**, 1725 (1993).
[23] J. F. Ziegler, J. P. Biersack, and U. Littmark, *The Stopping and Ranges of Ions in Solids* (Pergamon, New York, 1996).
[24] N. A. Tahir, Ph.D. thesis, Glasgow University, 1978.
[25] N. A. Tahir, K. A. Long, and E. W. Laing, J. Appl. Phys. **60**, 898 (1986).
[26] J. P. Christiansen, D. E. T. F. Ashby, and K. V. Roberts, Comput. Phys. Commun. **7**, 271 (1974).
[27] R. Ramirez *et al.*, Laser Part. Beams **16**, 91 (1998).
[28] N. A. Tahir and K. A. Long, Atomkernenergie **40**, 151 (1982).
[29] H. Bethe, Ann. Phys. (Leipzig) **5**, 325 (1930).
[30] J. Linhardt, M. Scharff, and H. E. Schott, Selsk. Mat. Fys Medd. **33** (14) (1963).
[31] M. D. Brown and C. D. Moak, Phys. Rev. B **6**, 90 (1972).